

Advanced X-Ray Diffraction

Corey Anderson

Thursday 6th July, 2023

Abstract

The rotating crystal method combined with Laue diffraction has emerged as a powerful technique for characterizing the structure of NaCl and LiF crystals. This investigation is aimed to determine the crystal orientations and lattice parameters of three NaCl crystals using this methodology. The results indicated that the rotating crystal method provided accurate and precise measurements, aligning well with theoretical predictions. However, the Laue diffraction technique displayed higher uncertainties, potentially stemming from errors in the production of the diffraction pattern. To enhance future experiments, it is recommended to slow down the rotation of the sample, allowing for the collection of additional data points in the lower resolution plots.

Contents

1 Theoretical Background	3
1.1 X-ray Generation	3
1.1.1 Braking Mechanism	3
1.1.2 The Auger Effect	3
1.1.3 Expected Spectrum	3
1.2 X-ray Diffraction	3
1.3 Rotating Crystal Method	4
1.4 Laue Diffraction	5
2 Aim	6
3 Methodology	6
3.1 Rotating Crystal Method	6
3.2 Laue Diffraction	6
4 Results	7
5 Discussion	8
5.1 Rotating Crystal Method	8
5.1.1 Crystal Orientations	8
5.1.2 Lattice Constant	9
5.1.3 Trends	9
5.2 NaCl Powder	10
5.3 Laue Diffraction	11
6 Conclusion	11
7 Appendix	11
7.1 Logbook	11
7.2 References	12

1 Theoretical Background

1.1 X-ray Generation

X-rays are generated from two mechanisms; Braking Mechanism and the Auger effect.

1.1.1 Braking Mechanism

A low voltage supply heats a filament, which ejects electrons which are accelerated by an electric field toward a copper target. When these electrons collide with the copper target, they are rapidly decelerated. This Deceleration of charged particles produces electromagnetic waves, in this case X-rays. This mechanism produces Bremsstrahlung X-rays of varying wavelengths.

1.1.2 The Auger Effect

This is a two step process. First, an inner shell electron is knocked out of the atom by an incoming electron. Second, an outer-shell electron drops to fill the inner shell vacancy, emitting its excess energy as an X-ray. However, the transition energy is a very precise amount and therefore this vacancy can only be filled by an electron dropping down from the M or L orbital as shown in Figure 1.

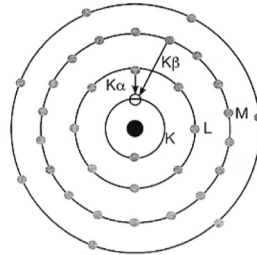


Figure 1: Atomic transitions responsible for the Auger emission peaks $K\alpha$ and $K\beta$.

1.1.3 Expected Spectrum

The braking mechanism generates Bremsstrahlung X-rays with varying wavelengths because the electrons have different kinetic energies before colliding with copper. This corresponds to a broad area on the spectrum. Conversely, the Auger Effect produces X-rays with specific wavelength because of the strict electron transitioning requirement. Since, there are two transitions possible, this corresponds to two sharp peaks on the spectra.

Since the electron in the M orbital transitions between a wider energy gap, the $K\beta$ is more energetic. However, the probability of the electron in the L orbital transitioning is higher since its energy gap is lower, so the $K\alpha$ peak has higher intensity.

1.2 X-ray Diffraction

X-rays can be diffracted by crystals because the interatomic distance in crystals is comparable to the X-ray wavelength.

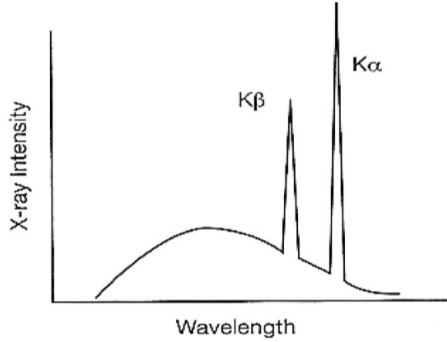


Figure 2: X-ray spectrum of copper featuring a smooth background due to Bremsstrahlung radiation and a pair of sharp peaks $K\alpha$ and $K\beta$ due to the Auger effect

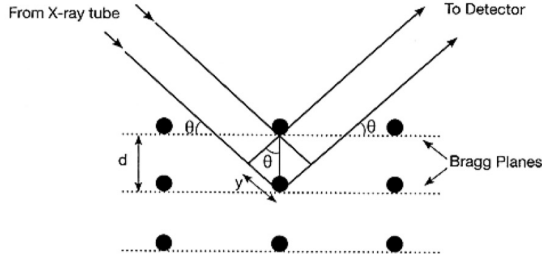


Figure 3: Bragg diffraction in a crystal lattice

For constructive interference to occur, the path difference between the two rays need to be an integer multiple of the wavelength. That is,

$$2d \sin \theta = n\lambda, \quad (1)$$

where $n = 1, 2, 3, \dots$ is the order of diffraction. This is known as Bragg's Law.

1.3 Rotating Crystal Method

From Bragg's Law, the peaks depend on the incident angle θ , we can obtain a spectrum by rotating the sample and observing the location of the peaks to multiple orders.

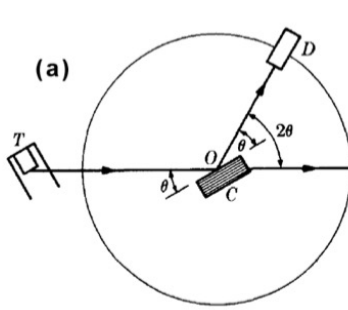


Figure 4: Varying θ allows us to observe multiple orders of diffraction

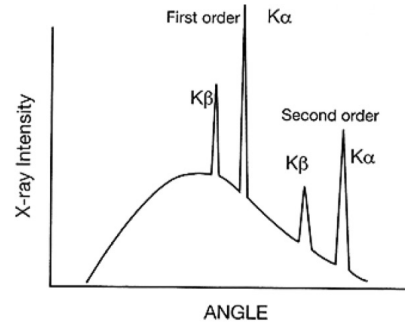


Figure 5: Expected Spectra featuring multiple orders of diffraction

1.4 Laue Diffraction

This method involves fixing the angle of the incident beam with respect to the crystal. According to Bragg's Law, there can only be one specific wavelength that results in diffraction. In order to observe multiple diffracted beams from different lattice planes, Laue diffraction involves the continuous (Bremsstrahlung) spectrum of X-ray radiation. The diffracted beams will hit the detection screen producing a spot at a distance L from the origin. If D is the distance between the crystal and the detection screen, the angle is given by:

$$\theta = \frac{1}{2} \tan^{-1} \left(\frac{L}{D} \right), \quad \text{where } L = \sqrt{y^2 + z^2}. \quad (2)$$

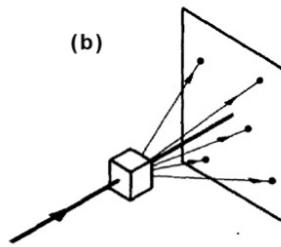


Figure 6: Multiple diffracted beams that result from Laue diffraction

2 Aim

To investigate how the structure and orientation of crystals affects the direction and intensity of diffracted x-rays.

3 Methodology

3.1 Rotating Crystal Method

1. Start the Measure Program
2. Calibrate the apparatus with the LiF sample
3. Input correct settings given by the operating instructions
4. Insert the sample to be measured
5. Start the measurement
6. After measurement has been completed, export the data as a text file
7. Repeat this for all 3 samples of NaCl, the NaCl powder and the KBr powder.

3.2 Laue Diffraction

1. Insert the LiF crystal into the machine
2. Record and process the Laue pattern
3. Find the values of y and z for each spot, use this to calculate θ .
4. Assign diffracted beams to a reflection from a particular lattice plane
5. Determine the d-spacing, and therefore the X-ray wavelength for each beam.

4 Results

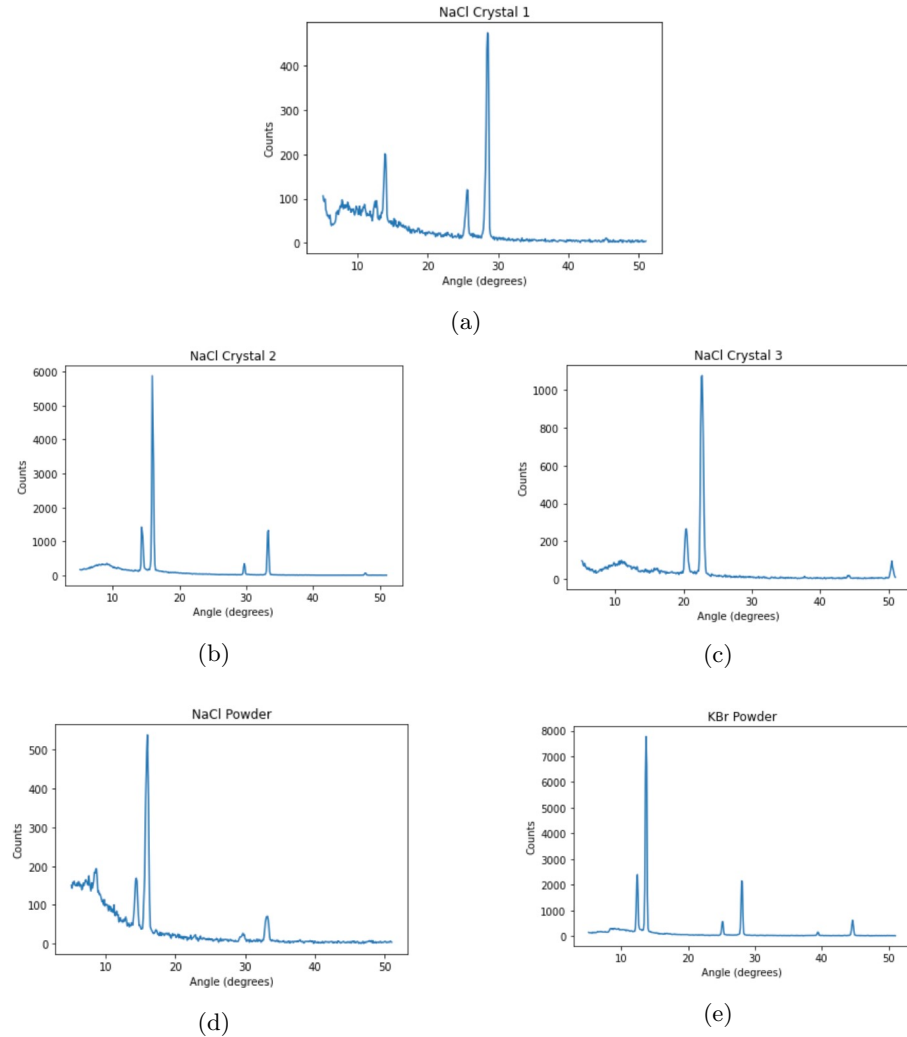


Figure 7: Spectra of crystals

Sample	Peak (°)	Onset (°)	Offset (°)	Uncertainty (\pm)
NaCl (I)	12.7	12.3	12.9	0.3
	13.9	13.5	14.3	0.4
	25.6	25.1	25.9	0.4
	28.5	27.8	28.9	0.6
NaCl (II)	14.4	14.3	14.6	0.2
	16.0	15.7	16.2	0.3
	29.7	29.6	29.8	0.1
	33.1	33.2	33.4	0.1
NaCl (III)	20.4	20.0	20.8	0.4
	22.7	22.2	23.3	0.6
	44.0	43.8	44.3	0.5
	50.5	50.3	50.7	0.2
NaCl Powder	14.4	13.9	14.8	0.6
	16.0	15.3	16.5	0.6
	29.5	29.3	29.8	0.3
	33.2	32.7	33.5	0.4
KBr Powder	12.4	12.1	12.7	0.3
	13.7	13.3	14.1	0.4
	28.0	27.7	28.3	0.3

Table 1: Crystal peak positions

5 Discussion

5.1 Rotating Crystal Method

The spectra is very similar to the expected spectrum (Figure 5). Interestingly, NaCl Powder and NaCl Crystal (I) did not have many counts recorded whereas NaCl Crystal 2 had plenty. Since the peaks are very narrow, the uncertainty was crudely calculated by taking half the difference between the onset and the offset.

5.1.1 Crystal Orientations

From Question 3, the possible orientations of the crystal based on the selection rules for a face centred Bravais Lattice has the h , k and l unmixed. At certain angles, we observe a maximum in the diffraction which is a peak in the spectra, the formula for calculating the angle is derived from Bragg's Law in the Appendix - Q3 as:

$$\theta = \sin^{-1} \left(\frac{\lambda \sqrt{h^2 + k^2 + l^2}}{2a} \right) \quad (3)$$

This results in the possible orientations and their corresponding angles:

Comparing Table 2 with Table 1, we find that:

NaCl (I) \rightarrow (111) orientation,

[100] orientation	[110] orientation	[111] orientation
200: $\theta_\alpha = 15.8^\circ, \theta_\beta = 14.3^\circ$	220: $\theta_\alpha = 22.7^\circ, \theta_\beta = 20.4^\circ$	111: $\theta_\alpha = 13.7^\circ, \theta_\beta = 12.3^\circ$
400: $\theta_\alpha = 33.1^\circ, \theta_\beta = 29.5^\circ$	440: $\theta_\alpha = 50.6^\circ, \theta_\beta = 44.2^\circ$	222: $\theta_\alpha = 28.2^\circ, \theta_\beta = 25.3^\circ$
		333: $\theta_\alpha = 45.2^\circ, \theta_\beta = 39.8^\circ$
		444: $\theta_\alpha = 71.1^\circ, \theta_\beta = 58.6^\circ$

Table 2: Possible orientation for a face centred Bravais Lattice

NaCl (II) \rightarrow (100) orientation,
 NaCl (III) \rightarrow (110) orientation.

The theoretical values align very accurately with the experimental values with most inside the uncertainty bounds. The (333) and (444) orientation peaks in NaCl crystal 1 was not observed possibly due to the low count number and thus the spectrum being in low resolution. This could be improved by setting the crystal increment to be 0.025° (1/4 of the value that was used).

The peaks in all spectra come in pairs: first one lower than the second. The lower one is $K\beta$ and the higher is $K\alpha$ for reasons provided in section 1.1.3. Each repetition of this pair is another order of diffraction, $n = 1, 2, 3, \dots$.

5.1.2 Lattice Constant

From Equation 3, we find that:

$$a = \frac{\lambda\sqrt{h^2 + k^2 + l^2}}{2\sin\theta}. \quad (4)$$

Each peak can give one estimate of a . So for each crystal we have 4 estimates in total. Averaging the 4 estimates for each crystal gives:

$$\begin{aligned} \text{NaCl (I)} &\rightarrow a = 5.55 \pm 0.06 \text{\AA} \\ \text{NaCl (II)} &\rightarrow a = 5.61 \pm 0.04 \text{\AA} \\ \text{NaCl (III)} &\rightarrow a = 5.65 \pm 0.05 \text{\AA} \end{aligned}$$

The uncertainties were calculated using propagation of uncertainty $\sigma_f = |\frac{df}{dx}| \sigma_x$. These estimates are all very close to the accepted value for NaCl, $a = 5.64 \text{\AA}$. The last two estimates fit within the uncertainty bounds but the first is outside of it. This is because of the low resolution spectrum of the first crystal, perhaps the X-rays from a (111) orientated crystal are not as likely to diffract toward the detector.

5.1.3 Trends

The trend in the peak intensity vs θ for the (100) and (110) crystals is such that the intensity of $K\alpha$ drops with every order (increase in θ). I hypothesise that this is due to the X-ray having to travel through a greater distance of the

crystal for higher orders and thus reducing the intensity. Another reason could be the 'Lambert's cosine law', which states that the intensity of radiation is proportional to the cosine of the angle between the direction of incidence and the normal to the surface. Hence, as the angle increases, the intensity decreases.

The (111) lattice does not follow this trend because unlike the other two orientations, all planes are possible (111), (222),..., since they do not involve the mixing of h , k and l . E.g. there is no Bragg peak from the (100) or (110) planes because this involves mixing of h , k and l .

5.2 NaCl Powder

From Table 1, we have the peaks with their attributes:

θ	Radiation	Orientation
14.4°	$K\beta$	(200)
16.0°	$K\alpha$	(200)
29.5°	$K\beta$	(400)
33.2°	$K\alpha$	(400)

Table 3: The attributes of the NaCl Powder peaks

My experimental spectrum for the NaCl powder had a maximum count of around 540. This is significantly less than the KBr spectrum that was recorded using research based apparatus; 7344 counts. This means that the quality of the my results is inferior due to the peaks having a lower resolution. Despite this, the peaks still aligned with the theoretical values (within uncertainty bounds). Interestingly, the spectrum taken for KBr during the lab (Plot (c)) had a similar count rate to the research acquired plot meaning that the NaCl powder is less effective than the KBr powder at diffracting the x-rays toward the detector.

5.3 Laue Diffraction

Type	θ_{exp}°	hkl	θ_{the}°	$ y/z - k/l $	d_{hkl} (pico)	λ (pico)
Bright Spot	14.6 ± 3.2	133	13.3	0.44	95	48 ± 10
Medium Spot 1	20.8 ± 1.9	244	19.5	0.94	69	49 ± 4
Medium Spot 2	23.2 ± 4.0	224	24.1	4.4	84.5	67 ± 11
Dim Spot 1	10.9 ± 1.6	133	13.3	0.031	95	36 ± 5
Dim Spot 2	16.8 ± 1.5	113	17.5	0.73	124.8	72 ± 6

Table 4: Angle of spots in Laue diffraction

Table 4 demonstrates that the longer the wavelength, the further out the diffraction pattern. It also suggests that the crystal orientation of LiF is (hll) with (133) being the most effective at diffraction. The quantities were calculated using the following formulas:

$$\lambda = 2d_{hkl} \sin \theta, \quad \text{where } d_{hkl} = \frac{a}{\sqrt{h^2 + k^2 + l^2}} \quad (5)$$

For a given lattice plane, $|y/z - k/l| \approx 0$. However, the medium spot 2 violates this rule, indicating a mistake in the assignment or the collection of data. As this data was collected by my lab partner, I am not able to analyse the errors during data collection. Diffraction would not be observed from the 200 plane because that implies $\theta = 90^\circ$, and since θ is the angle that the beam makes with the plane, that implies the beam hits the crystal and bounces back so it misses the detector. The lowest wavelength from the results is 36 ± 5 picometers so a wavelength of 33 picometers still fits in the uncertainty bound and is possible.

6 Conclusion

In conclusion, the rotating crystal method compared with Laue diffraction has proven to be a powerful technique for determining the structure of NaCl and LiF crystals. The orientations of the three NaCl crystals and the lattice parameters were determined to high accuracy and aligned with theoretical predictions well. However, it is worth noting that the Laue diffraction technique exhibited higher uncertainties in this particular experiment, which may be attributed to potential mistakes in producing the diffraction pattern. To improve future experiments, the rotation of the sample could be slowed to collect more data points for the lower resolution plots.

7 Appendix

7.1 Logbook

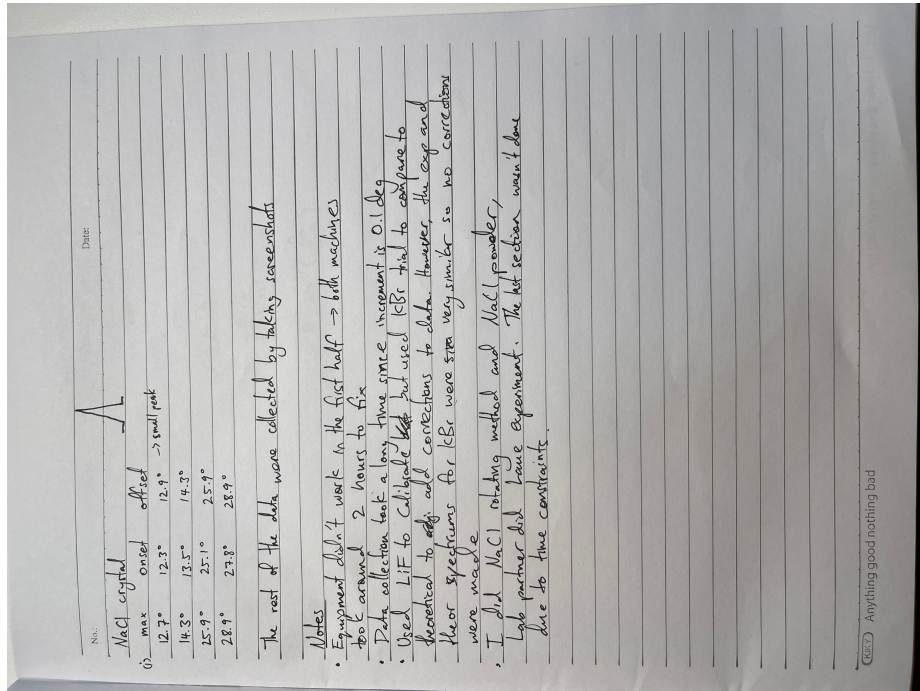


Figure 8

7.2 References

1. Crease, R.P., 2012. One amazing moment. Available at: <https://physicsworld.com/a/one-amazing-moment/>.
2. Kittel, C., 2004. Introduction to Solid State Physics. Wiley, pp.1-26.
3. Miller index notation. Available at: http://www.chem.qmul.ac.uk/surfaces/scc/scat1_1b.htm.
4. Cullity, B.D., 1956. Elements of X-Ray Diffraction. Addison-Wesley, pp.29-136.

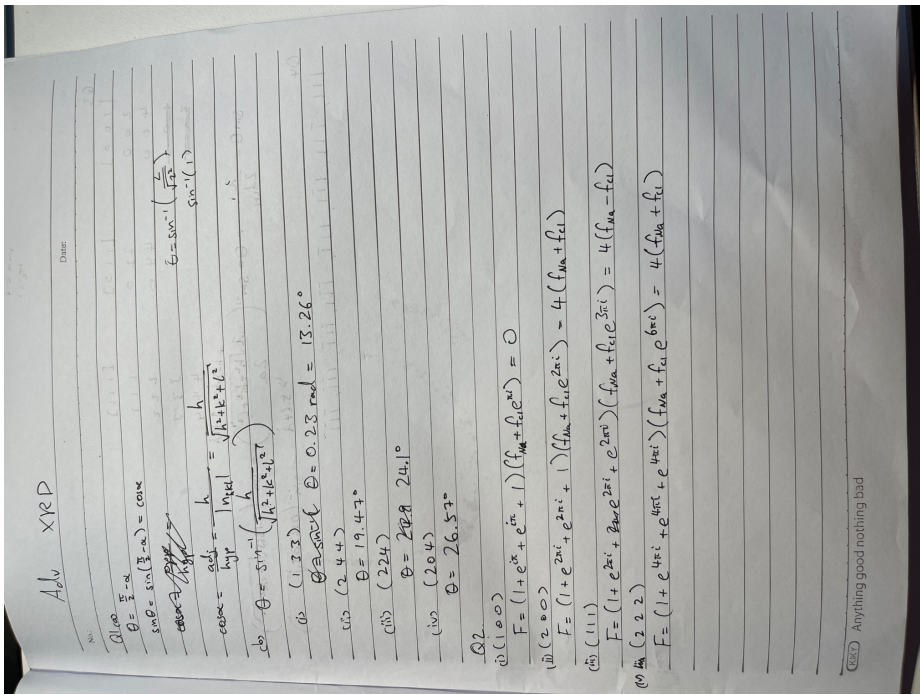


Figure 9

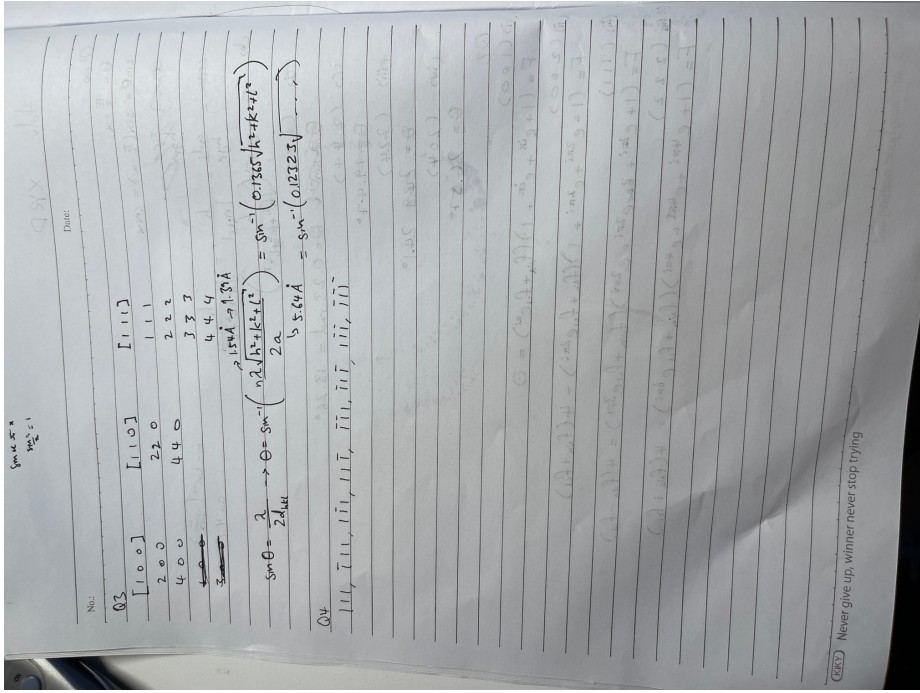


Figure 10

Line	hkl	2θ	θ	Intensity Parameters										Intensity %	
				$\sin\theta/\lambda$	f_K	f_{Br}	\pm	F	$ F ^2 \cdot p$	p	L-p	I(a.u)	Thy.	Exp.	
1	111	23.35	11.68	0.13	15.88	31.24	-	-61.42	3771.93	8.00	45.96	1386713.91	0.21	0.1748366	
2	200	27.05	13.53	0.15	15.30	30.18	+	181.89	33083.24	6.00	33.72	6693467.17	1.00	1	
3	220	38.65	19.33	0.21	13.76	26.82	+	162.31	26343.89	12.00	15.58	4924815.85	0.74	0.5360839	
4	311	45.60	22.80	0.25	12.28	25.60	-	-53.28	2838.76	24.00	10.76	733067.17	0.11	0.1373911	
5	222	47.80	23.90	0.26	12.00	25.22	+	148.85	22155.73	8.00	9.67	1714057.26	0.26	0.2181373	
6	400	55.75	27.88	0.30	10.97	23.81	+	139.14	19358.83	6.00	6.81	791499.69	0.12	0.1824619	
7	331	61.20	30.60	0.33	10.31	22.86	-	-50.23	2523.45	24.00	5.52	334555.95	0.05	0.0800654	
8	420	63.00	31.50	0.34	10.10	22.56	+	130.62	17062.63	24.00	5.18	2121813.37	0.32	0.2602124	
9	422	69.80	34.90	0.37	9.54	21.68	+	124.88	15594.02	24.00	4.17	1560202.78	0.23	0.1542756	
10	333	74.75	37.38	0.39	9.06	20.97	-	-47.64	2269.95	8.00	3.65	66305.31	0.01	0.0709423	
11	440	82.70	41.35	0.43	8.77	20.93	+	118.82	14117.24	12.00	3.10	525382.31	0.08	0.0880991	
12	600	88.95	44.48	0.45	8.29	19.56	+	111.39	12407.29	6.00	2.86	212621.86	0.03	0.1092048	

Figure 11: Question 5